Diagn Interv Radiol 2007; 13:3-9

NEURORADIOLOGY

ORIGINAL ARTICLE

Evaluation of cerebral glioma grade by using normal side creatine as an internal reference in multi-voxel ^{1}H-MR spectroscopy

Hasan Yerli, Ahmet Muhteşem Ağıldere, Özlem Özen, Elif Geyik, Başar Atalay, Atilla Halil Elhan

PURPOSE

Our purpose was to evaluate cerebral glioma grade by using normal side creatine (Cr) as an internal reference in multi-voxel ^{1}H-MR spectroscopy.

MATERIALS AND METHODS

We examined 25 adult patients with glial brain tumors. Ratios of maximum Cho/Cr_{normal} (max-Cho/Cr_n) and minimum NAA/Cr_{normal} (min-NAA/Cr_n) were determined using Cr levels in the normal parenchyma. In addition, maximum Cho/Cr (max-Cho/Cr) and minimum NAA/Cr (min-NAA/Cr) were calculated from spectrum in the tumor areas. Tumors were graded according to metabolite ratios and the findings were compared to histopathological test results. The sensitivity, specificity, positive and negative predictive values of metabolite ratios were determined.

RESULTS

The ratio of max-Cho/Cr_n was lower than that of max-Cho/Cr in the high-grade group (P = 0.001). Min-NAA/Cr_n, min-NAA/Cr, and max-Cho/Cr ratios demonstrated statistically significant differences between high-grade (n = 19) and low-grade tumors (n = 6). The min-NAA/Cr and min-NAA/Cr_n ratios were inversely correlated with tumor grade (P = 0.027 and P = 0.009, respectively).

CONCLUSION

Use of normal side Cr as an internal reference provides a more objective evaluation for brain tumor grading. Our data showed that Cr tended to be low in the high-grade tumors. In addition to conventional metabolite ratios, the Min-NAA/Cr_n ratio might be useful in brain tumor grading. Combined use of metabolite ratios might be helpful in grading brain tumors in cases without significantly increased Cho/Cr ratios.

Key words: • *magnetic resonance spectroscopy* • *brain* • *neoplasm*

From the Departments of Radiology (H.Y. ✉ *hasanyerli@yahoo.com*, A.M.A., E.G.), Pathology (Ö.Ö.), and Neurosurgery (B.A.), Başkent University School of Medicine, Ankara, Turkey; and Department of Biostatistics (A.H.E.), Ankara University School of Medicine, Ankara, Turkey.

Received 21 December 2006; revision requested 8 January 2007; revision received 16 January 2007; accepted 17 January 2007.

It is important to determine brain tumor grade before establishing effective therapy. Although conventional magnetic resonance imaging (MRI) is a useful method (1, 2), it is not always possible to determine brain tumor grade (3, 4). Several noninvasive neuroimaging methods, including proton magnetic resonance spectroscopy imaging (^{1}H-MRS), diffusion-weighted MRI, and perfusion MRI, have been used to determine brain tumor grade (3, 5–7). Numerous studies have shown that ^{1}H-MRS improves preoperative diagnosis of brain tumor grading, although the accuracy of noninvasive advanced neuroimaging methods is controversial (3, 5, 8–10). Further investigations have been recommended to increase the clinical utility of these methods (5, 9).

^{1}H-MRS provides data related to biochemical changes in the tumor and may therefore help in predicting brain tumor grade as a noninvasive diagnostic tool. Choline (Cho) is known as a radiological marker suggesting cell turnover. Brain tumors mostly demonstrate elevation in the ratio of Cho/Creatine (Cr); however, glial neoplasms without elevated Cho/Cr ratios also have been reported (11–13). N-acetyl aspartate (NAA) decreases in any disease associated with loss of neurons. Cr metabolite reflects information on energy metabolism. Results of several studies suggest, surprisingly, that levels of Cr are the same in both low- and high-grade gliomas (14, 15). Nonetheless, previous studies have pointed out that decreased Cr levels can be seen in brain tumors (16, 17). Additionally, the amount of Cr may be variable in different regions of the same tumor. Elevated Cr may be seen in the hypometabolic areas and decreased Cr may be observed in the hypermetabolic areas of the same tumor (4, 18). The importance of Cr levels is not clear in the differentiation of low- and high-grade gliomas. If the Cr signal in the tumor area is used as an internal standard, it may be difficult to identify differences in metabolite ratios and it also might cause errors in predicting tumor grade.

In this study, we used the metabolite of Cr from the symmetrical normal brain area as a normal reference peak. We calculated both the ratios of tumor main metabolites to Cr from contralateral normal brain parenchyma and the ratios of tumor main metabolites to each other, semiquantitatively. Our purpose was to evaluate cerebral glioma grade by using normal side Cr as an internal reference in multi-voxel ^{1}H-MRS to avoid the problems of using Cr as a reference peak from the tumor area.

Materials and methods

Patient population

This study was approved by the ethics committee of our hospital and informed consent was obtained from all patients. The 30-month prospective study included 25 consecutive adult patients (aged between

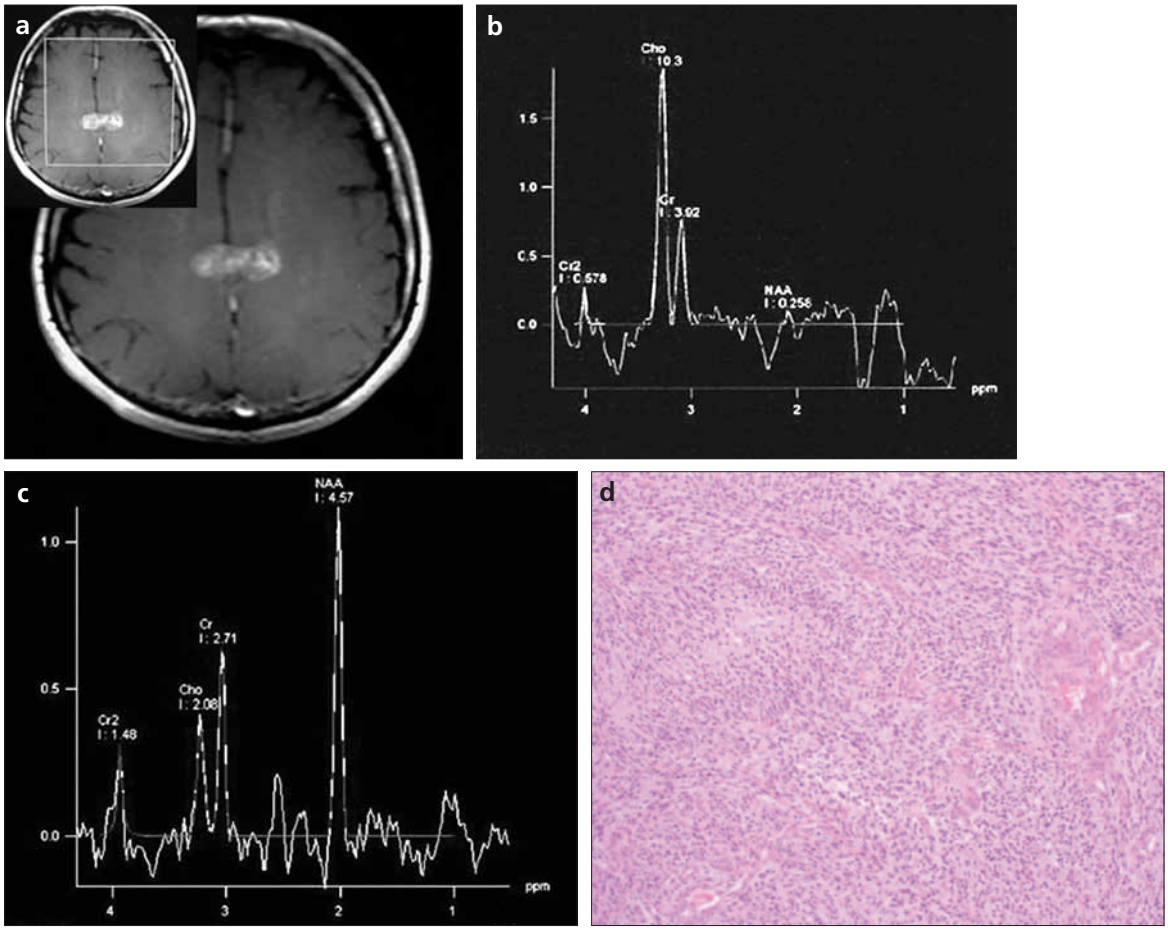

Figure 1. a-d. A 54-year-old woman with glioblastoma multiforme. Post-contrast axial T1-weighted MR image **(a)** shows strong contrast enhancement crossing the corpus callosum and midline. Spectra from the tumor area **(b)** and normal cerebral hemisphere **(c)** show markedly decreased NAA/Cr (0.07) and NAA/Cr_n (0.10) ratios, and markedly increased Cho/Cr ratio (2.63). These findings appear to be consistent with a high-grade tumor. Pathologic specimen **(d)** shows microvascular proliferation, high cellularity, and necrosis with pseudopalisading of tumor cells (HE; x10, original magnification).

22–79 years; mean age, 47 years) with glial brain tumors (19 high-grade and 6 low-grade). Among the patients, 21 did not have any therapeutic or diagnostic intervention before MRI examinations, and 4 patients (2 low-grade, 2 high-grade) underwent stereotactic biopsy before MRI examinations, but none of them had any therapy before ^{1}H-MRS. All patients were diagnosed histopathologically after tumor resection (n = 19 patients) or stereotactic biopsy (n = 6). The biopsy targets were determined by a radiologist and a neurosurgeon.

Conventional MRI

All MRI scans were performed using a 1.5 T MR system with a head coil (Symphony, Siemens, Erlangen, Germany). Routine brain MRI was performed with T1-weighted (TR/TE, 575/15 ms), T2-weighted turbo spin-echo (TR/TE, 5160/103 ms), and FLAIR (TR/TE/TI, 9000/110/2500 ms) images in the axial plane, and T2-weighted turbo spin-echo images in the coronal plane (TR/TE, 4510/112 ms). In addition, axial (TR/TE, 911/15 ms), coronal (TR/TE, 839/15 ms), and sagittal fat-suppressed (TR/TE, 903/14 ms) T1-weighted images with 5 mm slice thickness were obtained after intravenous injection of 0.1 mmol/kg gadolinium compound.

Multi-voxel ^{1}H-MRS imaging

Multi-voxel ^{1}H-MRS was performed with a 2D chemical shift imaging (CSI) technique, with CSI-SE volume preselection. ^{1}H-MRS scanning was obtained after gadolinium administration (Fig. 1). FLAIR and T2-weighted MR images were used as references for the lesions that did not demonstrate contrast enhancement (Figs. 2, 3).

^{1}H-MRS was performed before treatment to avoid the effects of radiation, surgery, or chemotherapy, and automated shimming and water suppression were used. The scanning volume included both the tumor region and the normal-appearing symmetric contralateral brain region, depending on lesion size, for each case. The scanning parameters were as follows: field of view, 16 × 16 cm; phase encoding matrix, 16 × 16; TE, 135 ms; TR, 1500 ms; NEX, 4; voxel size, 1 cm^3; acquisition time, 6.5 min.

To prevent contamination of the spectra from scalp fat, normal brain parenchyma, partial volume of bone, cerebrospinal fluid, and paranasal sinus aeration, the volume of interest was completely enclosed within the brain. To assure spectral quality, the metabolite ratios from the tumor area were compared to the ratios obtained from normal-appearing contralateral brain parenchyma. Cr peak in the normal contralateral symmetric brain parenchyma was used as an internal stand-

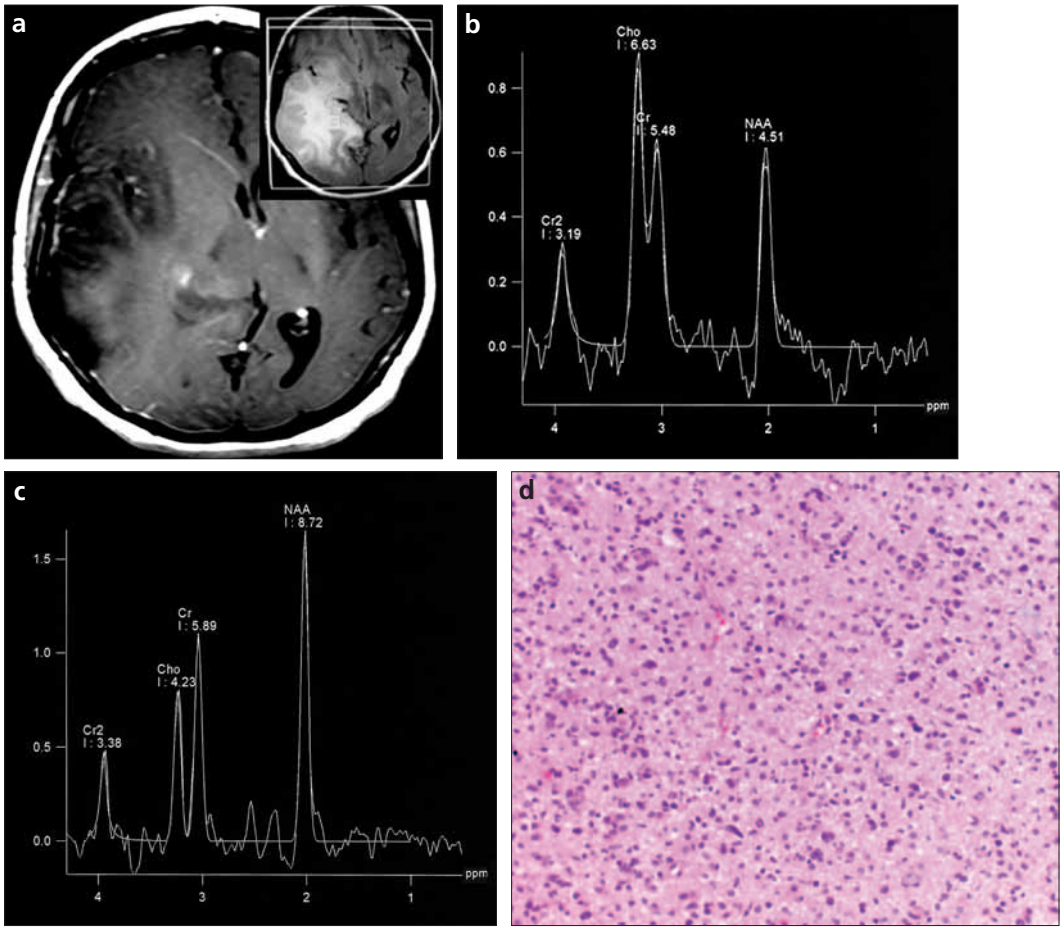

Figure 2. a-d. A 28-year-old woman with grade II astrocytoma. Post-contrast axial T1-weighted MR image **(a)** demonstrates minimal contrast enhancement involving the tumor area. Spectra from the tumor area **(b)** and symmetric normal cerebral hemisphere **(c)** show slightly decreased NAA/Cr (0.82) and NAA/Cr_n (0.76) ratios, and slightly increased Cho/Cr (1.2) ratio (1.12). These findings are consistent with a low-grade tumor. Pathologic specimen **(d)** shows intermediate cellularity and prominent nuclear pleomorphism (HE; x20, original magnification).

ard peak to investigate changes in the tumors' metabolites.

Postprocessing was performed using a workstation with standard software (Leonardo, Siemens Medical Systems, Malvern, PA, USA). After automated postprocessing of ^{1}H-MRS data, Cho (at 3.22 ppm), Cr (at 3.02 ppm), NAA (at 2.02 ppm), lipids (at 0.8-1.3 ppm), and lactate (at 1.3 ppm) were identified. The ratios of maximum Cho/Cr_{normal} (max-Cho/Cr_n) and minimum NAA/Cr_{normal} (min-NAA/Cr_n) were calculated using Cr levels in the contralateral normal brain parenchyma. In addition, conventional max-Cho/Cr and min-NAA/Cr ratios were obtained from spectra in the solid tumor areas. ^{1}H-MRS analysis was performed by observers that were blinded to the final histopathological diagnoses of the tumors. The abbreviations used in this article are shown in Table 1. All ratios were compared with their normal ratios in normal-appearing contralateral brain parenchyma.

Histopathological evaluation

The tissues used in this study were formaldehyde-fixed and paraffin-embedded specimens obtained from patients who had brain tumors. In each case, the histopathological diagnosis was established by standard light-microscopic evaluation of sections stained with hematoxylin and eosin. The sections of each neoplasm were evaluated using World Health Organization (WHO) criteria for brain tumor classification (19). According to this system, pilocytic astrocytomas (n = 2) were classified as grade I, diffuse astrocytomas (n = 3) and oligodendroglioma (n = 1) as grade II; anaplastic astrocytomas (n = 5), anaplastic oligodendroglioma (n = 1), and anaplastic oligoastrocytoma (n = 1) as grade III, and glioblastoma multiforme (n = 11) and gliosarcoma (n = 1) as grade IV. Ki-67 proliferation indices were immunohistochemically established for each tumor.

Statistical analysis

Comparisons of median metabolite ratios between low- and high-grade tumors were analyzed using the Mann-Whitney U test. Differences for paired comparisons were evaluated by Wilcoxon signed ranks test. The sensitivity, specificity, positive predictive value (PPV), and negative predictive value (NPV), as well as related cutoffs of different metabolite ratios, were calculated. High-grade tumors were regarded as true positive, and low-grade tumors were considered true negative. Receiver operating characteristic (ROC) curves were used to describe and compare the performance of the diagnostic values of the metabolite ratios. The area under the ROC curve gives an estimate of the overall accuracy of each metabolite

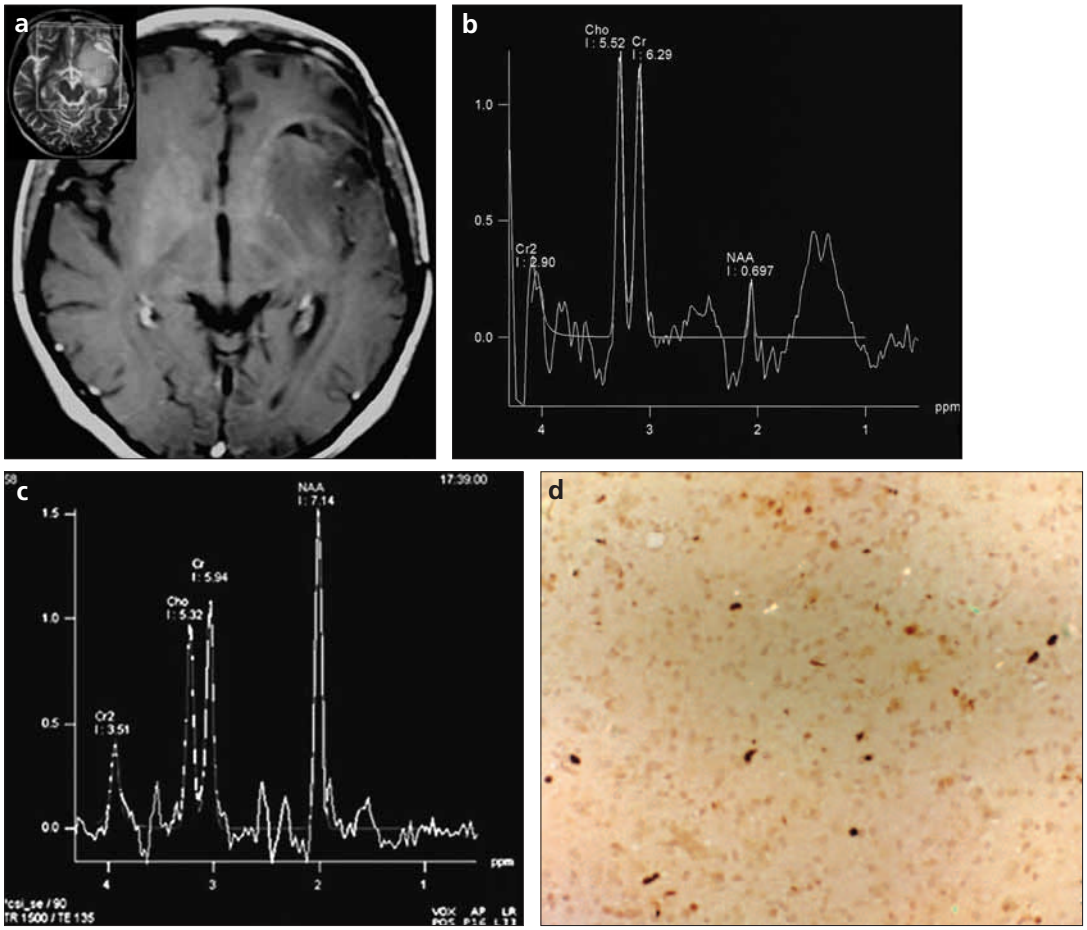

Figure 3. **a-d.** A 26-year-old woman with anaplastic astrocytoma. Post-contrast axial T1-weighted MR image **(a)** demonstrates decreased signal intensity without contrast enhancement involving the left basal ganglion, the insular cortex, and the frontal lobe in the left cerebral hemisphere. The lesion was initially considered as a low-grade tumor, owing to minimal edema, the lack of contrast enhancement, and necrosis. Spectra from the tumor area **(b)** and symmetric normal cerebral hemisphere **(c)** demonstrate markedly decreased NAA/Cr (0.11) and NAA/Cr_n (0.12) ratios. These findings are consistent with a high-grade tumor, although the Cho/Cr ratio (0.87) appears to be within normal limits. Pathologic specimen **(d)** shows relatively low cellularity (Ki-67 labeling index was 4%) (immunoperoxidase; × 20, original magnification).

ratio. An area of 0.50 implies that the variable adds no information, whereas an area of 1 implies perfect accuracy. The areas under the ROC curves for all variables were calculated as described by Hanley and McNeil (20, 21). We assessed whether the difference in the areas under 2 curves was random or real by calculating a critical ratio, z (AccuROC for Windows, Version 2.5, Accumetric Corp, Montreal, Quebec, Canada). *P* values < 0.05 were considered statistically significant. Statistical analyses were performed using SPSS software (Statistical Package for the Social Sciences, Version 11.5, SPSS Inc, Chicago, IL, USA).

Results

Ratios of metabolites according to tumor grade are shown in Table 1. The ratio of max-Cho/Cr_n was significantly lower than that of max-Cho/Cr in the high-grade group (P = 0.001). Max-Cho/Cr, min-NAA/Cr, and min-NAA/Cr_n ratios demonstrated a statistically significant difference between high- and low-grade tumors (P = 0.007, 0.027, and 0.009, respectively). Both max-Cho/Cr_n and max-Cho/Cr ratios in the high- and low-grade tumors were higher than that of normal Cho/Cr ratios.

Although the ratio of min-NAA/Cr_n was lower than that of min-NAA/Cr in the low- and high-grade groups, these differences were not statistically significant (P = 0.917 and P = 0.065, respectively). The median max-Cho/Cr (2.45) and max-Cho/Cr_n (1.34) ratios were higher in high-grade tumors than in low-grade tumors. The median min-NAA/Cr ratio (0.32) and median min-NAA/Cr_n ratio (0.19) were found to be lower in high-grade tumors than in low-grade tumors (Table 1). The Cho/Cr and NAA/Cr ratios for normal-appearing contralateral brain areas are shown in Table 1.

Lactate peaks were found more frequently in high-grade tumors than in low-grade tumors (P = 0.002). There was no statistically significant difference between high- and low-grade tumors in terms of lipid peaks (P = 0.363).

The area under the ROC curves revealed that each metabolite ratio proved to be significantly powerful in predicting tumor grading, except for max-Cho/Cr_n (Table 2). The min-NAA/Cr and min-NAA/Cr_n ratios were correlated inversely with tumor grading. An inverse correlation was more prominent with min-NAA/Cr_n. The max-Cho/Cr ratios correlated positively with tumor grading. The sensitivity, specificity, PPV, and NPV, together with cutoffs, are shown in Table 2.

Discussion

Conventional MRI is an important method in brain tumor grading (1, 2), but MRI-based tumor grading is sometimes limited and may lead to low- or high-grade misclassification in some cases (2, 3) (Fig. 2). In general, the ^{1}H-MRS technique cannot eliminate the need for a biopsy and histopathological confirmation; however, in some patients, operation is not possible due to impaired clinical condition and ^{1}H-MRS provides data related to biochemical changes in the tissue and may therefore be beneficial, at least in assessing the tumor entity (22). CSI has the advantage of using multiple spectra from multiple contiguous voxels; both the tumor itself and the adjacent tissue, and other brain areas that may appear unremarkable in conventional MRI can be evaluated. It is reported that perfusion and diffusion MRI can also be helpful tools for the discrimination of glial tumor grades, and these tools may be combined to increase diagnostic accuracy (3, 6, 23–29).

The Cr peak includes Cr and phosphocreatine. Cr is a metabolite that provides phosphate through phosphocreatine for adenosine triphosphate (ATP) and has a critical function in the cell energy system (4, 8, 14). Levels of Cr in glioma tumors are controversial. In a study by Stadlbauer et al., there were no significant differences in tumor Cr between grade I and grade II gliomas; however, they found higher values of the Cr in grade III astrocytomas compared to other grade III gliomas, including oligodendrogliomas and oligoastrocytomas (14). Likavcanova et al. studied the metabolism of gliomas and found that the levels of Cr were the same in low- and high-grade gliomas (15). A reason for the varying results might be the heterogenous histological and metabolic nature of gliomas (14, 30). In our study, the ratio of max-Cho/Cr_n was lower than that of max-Cho/Cr in the high-grade group (P = 0.001). This result points out that lower Cr levels might have been present in our high-grade tumor population. If Cr signal in the tumor area is regarded as the sole internal reference, the calculated ratio would not reliably reflect the amount of the metabolite tested. On the other hand, Cr is relatively constant in normal brain regions and it is considered an internal standard (7, 31).

Yang et al. determined that there were no significant differences between max-Cho/Cr_n ratios in glioblastoma and anaplastic gliomas in 17

Table 1. Metabolite ratios according to tumor grade

	Low-grade (grade I-II) n = 6		High-grade (grade III-IV) n = 19		
	Mean ± SD	Median (min-max)	Mean ± SD	Median (min-max)	*P* value
max-Cho/Cr	1.75 ± 0.29	1.7 (1.4-2.28)	3.03 ± 2.34	2.45 (0.87-12.50)	0.007
max-Cho/Cr_n	1.4 ± 0.64	1.2 (0.4-2.29)	1.65 ± 0.82	1.34 (0.57-3.01)	0.525
min-NAA/Cr	0.64 ± 0.25	0.6 (0.28-1.06)	0.37 ± 0.28	0.32 (0.06-1.13)	0.027
min-NAA/Cr_n	0.58 ± 0.18	0.50 (0.37-0.80)	0.29 ± 0.23	0.19 (0.03-0.80)	0.009
Normal ratios					
Cho/Cr	0.97 ± 0.41	0.85 (0.50-1.67)	1.01 ± 0.22	0.99 (0.66-1.52)	0.542
NAA/Cr	1.49 ± 0.56	1.8 (0.62-2.05)	1.61 ± 0.52	1.55 (0.90-3.08)	0.803

SD: standard deviation; min: minimum; max: maximum; n: number
max-Cho/Cr: maximum tumor choline/tumor creatine ratio
max-Cho/Cr_n: maximum tumor choline/normal creatine ratio
min-NAA/Cr: minimum tumor N-acetyl aspartate/tumor creatine ratio
min-NAA/Cr_n: minimum tumor N-acetyl aspartate/normal creatine ratio
Cho/Cr: normal choline/creatine ratio
NAA/Cr: normal N-acetyl aspartate/creatine ratio

Table 2. Sensitivity, specificity, PPV, and NPV of different metabolite ratios in predicting tumor grade

	Cutoff	Sensitivity	Specificity	PPV	NPV	AUC ± SE
max-Cho/Cr	2	0.85	0.86	0.94	0.67	0.850 ± 0.075
max-Cho/Cr_n	1.95	0.40	0.86	0.89	0.33	0.582 ± 0.119[a]
min-NAA/Cr	0.5	0.75	0.86	0.94	0.55	0.786 ± 0.091
min-NAA/Cr_n	0.44	0.80	0.86	0.94	0.60	0.839 ± 0.076

PPV: positive predictive value; NPV: negative predictive value; AUC: area under curve; SE: standard error
[a] Not statistically significant.
max-Cho/Cr: maximum tumor choline/tumor creatine ratio
max-Cho/Cr_n: maximum tumor choline/normal creatine ratio
min-NAA/Cr: minimum tumor N-acetyl aspartate/tumor creatine ratio
min-NAA/Cr_n: minimum tumor N-acetyl aspartate/normal creatine ratio

patients with gliomas (7); however, they found that there were significant differences between the high- and low-grade gliomas for max-Cho/Cr_n ratio. In our study, max-Cho/Cr_n ratios were slightly different than those presented by Yang et al. Although the ratios of max-Cho/Cr_n were elevated in both low- and high-grade gliomas when compared with that of the symmetric normal voxel, this relationship was not statistically significant. In other words, max-Cho/Cr_n ratio may not be helpful in differentiation of low- and high-grade gliomas. The max-Cho/Cr_n ratio may not be adequate for tumor grade differentiation because Cho signals can correlate with tumor cellularity, but tumor cellularity cannot directly reflect tumor grade. Mitotic activity, necrosis, and vascular proliferation are the most important parameters in the histopathological differentiation of tumor grade (3, 21). Both low- and high-grade gliomas can cause high cell membrane turnover, and using only the comparison of Cho signal without the contribution of decreased tumor Cr signal might be inadequate for making the diagnosis of glioma grading. Hence, max-Cho/Cr ratio might be more valuable than max-Cho/Cr_n ratio for grading of gliomas. Nevertheless, contralateral normal Cr may be used for more objective evaluation of tumor Cho and Cr signals (31). The results of our study might have also been affected by the heterogeneity of cases within the group of low- and high-grade tumors, because it has been reported that glial tumors with an oligodendrocytic component tend to demonstrate a more pronounced increase in Cho and Cr than astrocytomas do (32). Larger series with greater numbers of astrocytomas and glial tumors with an oligodendrocytic component are needed to evaluate the accuracy of metabolite ratios for these tumor groups.

It has been reported that treated brain tumors have relatively lower Cho levels compared to untreated tumors (29, 33). Three case reports regarding untreated glial tumors demonstrated no significant increase in Cho peak or Cho/Cr ratio (11–13). It was thought that this scenario might be related to the non-proliferative phase of the cell cycle. In our study, we determined one anaplastic astrocytoma case with low NAA/Cr_n and NAA/Cr ratios. This case did not demonstrate an increased Cho/Cr ratio (Fig. 3). This was most probably due to high NAA destruction in the tumor area and the non-proliferative phase of the cell cycle. To minimize the pitfalls of the evaluation of unusual MR spectra, all brain metabolites should be evaluated together in tumor grading.

Stadlbauer et al. found a negative linear correlation between the total tumor NAA and the degree of tumor infiltration (14). The most malignant features of the tumor define grade of glioma. It can be considered that the destruction of the NAA metabolite is maximal in the most malignant regions of the tumor and minimal NAA-related metabolite ratios (min-NAA/Cr_n and min-NAA/Cr) associated with neuron destruction and necrosis might reflect the most malignant portion, and therefore, grade of the tumor. On the basis of our results, the min-NAA/Cr_n ratio appears to be a good parameter for determining glioma grade. We think that NAA destruction may be significant, although the decreased anabolism of tumor cells may cause a slightly increased Cho signal with low cell membrane proliferation (Fig. 3). As a result, min-NAA/Cr_n ratio might be more reliable than max-Cho/Cr_n ratio for glioma grading.

Several studies have demonstrated that myo-inositol, lipid, and lactate can be markers of tumor malignancy (4, 5, 7, 34). We determined that there was a strong correlation between lactate and tumor grade. The results of our study are in good agreement with previous studies; however, we did not identify a statistically significant difference between high- and low-grades tumors based on lipid signal. This result was probably the outcome of the effect of noise. Lipid peak, which can be seen as a broad peak, might be interfered with by noise (35). We did not evaluate myo-inositol levels. It is known that a short TE sequence is more sensitive in detecting myo-inositol (34).

One potential limitation of our study was the small number of patients with low-grade tumors. Our study was also limited by the fact that we calculated metabolite ratios semiquantitatively. We did not calculate molar metabolite concentrations.

To conclude, the use of normal side Cr as an internal reference provides a more objective evaluation for brain tumor grading. In our study, Cr tended to be low in the high-grade tumor area, and such a decrease plays an important role in brain tumor grading. From this point of view, Cr signals from normal-appearing contralateral brain areas can be used as an internal reference for the tumor metabolites. Min-NAA/Cr_n as well as max-Cho/Cr and min-NAA/Cr ratios might be useful in brain tumor grading. Some malignant brain tumors did not demonstrate a marked increase in Cho/Cr ratios, probably due to low tumor cell proliferative activity. This pitfall should be considered as well as that evaluation of all metabolite ratios might be useful in predicting brain tumor grade.

References

1. Dean BL, Drayer BP, Bird CR, et al. Gliomas: classification with MR imaging. Radiology 1990; 174: 411–415.
2. Lee J, Yamaguchi T, Abe A, et al. Clinical evaluation of choline measurement by proton MR spectroscopy in patients with malignant tumors. Radiat Med 2004; 22:148–154.
3. Law M, Yang S, Wang H, et al. Glioma grading: sensitivity, specificity and predictive values of perfusion MR imaging and proton MR spectroscopic imaging compared with conventional MR imaging. AJNR Am J Neuroradiol 2003; 24: 1989–1998.
4. Li X, Lu Y, Pirzkall A, McKnight T, Nelson SJ. Analysis of the spatial characteristics of metabolic abnormalities in newly diagnosed glioma patient. J Magn Reson Imaging 2002; 16: 229–237.
5. Bulakbasi N, Kocaoglu M, Ors F, Tayfun C, Ucoz T. Combination of single-voxel proton MR spectroscopy and apparent diffusion coefficient calculation in the evaluation of common brain tumors. AJNR Am J Neuroradiol 2003; 24: 225–233.
6. Henry RG, Vigneron DB, Fischbein NJ, et al. Comparison of relative cerebral blood volume and proton spectroscopy in patient with treated gliomas. AJNR Am J Neuroradiol 2000; 21: 357–366.
7. Yang D, Krogi Y, Sugahara T, et al. Cerebral gliomas: prospective comparison of multivoxel 2D chemical-shift imaging proton MR spectroscopy, echo planar perfusion and diffusion-weighted MRI. Neuroradiology 2002; 44: 656–666.
8. Burtscher IM, Holtas S. Proton magnetic resonance spectroscopy in brain tumors: clinical applications. Neuroradiology 2001; 43:345–352.
9. Nelson SJ, McNight TR, Henry RG. Characterization of untreated gliomas by magnetic resonance spectroscopic imaging. Neuroimag Clin N Am 2002; 12:599–613.
10. Tzika AA, Vajapeyam S, Barnes PD. Multivoxel proton MR spectroscopy and hemodynamic MR imaging of childhood brain tumors: preliminary observations. AJNR Am J Neuroradiol 1997; 18:203–218.
11. Londono A, Castillo M, Armao D, Kwock L, Suziki K. Unusual MR spectroscopic imaging pattern of an astrocytoma: lack of elevated choline and high myo-inositol and glycine levels. AJNR Am J Neuroradiol 2003; 24:942–945.

12. Mohana-Borges AV, Imbesi SG, Dietrich R, Alksne J, Amjadi DK. Role of proton magnetic resonance spectroscopy in the diagnosis of gliomatosis cerebri: a unique pattern of normal choline but elevated myo-inositol metabolite levels. J Comput Assist Tomogr 2004; 28:103–105.
13. Saraf-Lavi E, Bowen BC, Pattany PM, Sklar EM, Murdoch JB, and Petito CK. Proton MR spectroscopy of gliomatosis cerebri: case report of elevated myoinositol with normal choline levels. AJNR Am J Neuroradiol 2003; 24:946–951.
14. Stadlbauer A, Gruber S, Nimsky C, et al. Preoperative grading of gliomas by using metabolite quantification with high-spatial-resolution proton MR spectroscopic imaging. Radiology 2006; 238:958–969.
15. Likavcanova K, Dobrota D, Liptaj T, et al. In vitro study of astrocytic tumour metabolism by proton magnetic resonance spectroscopy. Gen Physiol Biophys 2005; 24:327–335.
16. Isobe T, Matsumura A, Anno I, et al. Quantification of cerebral metabolites in glioma patients with proton MR spectroscopy using T2 relaxation time correction. Mag Reson Imaging 2002; 20:343–349.
17. Tong Z, Yamaki T, Harada K, Houkin K. In vivo quantification of the metabolites in normal brain and brain tumors by proton MR spectroscopy using water as an internal standard. Magn Reson Imaging 2004; 22:1017–1024.
18. Alger JR, Frank JA, Bizzi A, et al. Metabolism of human gliomas: assessment with H-1 MR spectroscopy and F-18 fluorodeoxyglucose PET. Radiology 1990; 177:633–641.
19. Kleihues P, Louis DN, Scheithauer BW, et al. The WHO classification of tumors of the nervous system. J Neuropathol Exp Neurol 2002; 61:215–229.
20. Hanley JA, McNeil BJ. The meaning and use of the area under a receiver operating characteristic (ROC) curve. Radiology 1982; 143:29–36.
21. Hanley JA, McNeil BJ. A method of comparing the areas under receiver operating characteristic curves derived from the same cases. Radiology 1983; 148:839–843.
22. Law M. MR spectroscopy of brain tumors. Top Magn Reson Imaging 2004; 15:291–313.
23. Graves EE, Nelson SJ, Vigneron DB, et al. Serial proton MR spectroscopic imaging of recurrent malignant gliomas after gamma knife radiosurgery. AJNR Am J Neuroradiol 2001; 22:613–624.
24. Li Belinda SY, Babb JS, Soher BJ, Maudsley AA, Gonen O. Reproducibility of 3D proton spectroscopy in the human brain. Magn Reson Med 2002; 47:439–446.
25. McKnight TR, Noworolski SM, Vigneron DB, Nelson SJ. An automated technique for the quantitative assessment of 3D-MRSI data from patient with glioma. J Magn Reson Imaging 2001; 13:167–177.
26. Schlemmer HP, Bachert P, Herfarth KK, Zuna I, Debus J, Van Kaick G. Proton MR spectroscopic evaluation of suspicious brain lesions after stereotactic radiotherapy. AJNR Am J Neuroradiol 2001; 22:1316–1324.
27. Butzen J. Prost R, Chetty V, et al. Discrimination between neoplastic and nonneoplastic brain lesions by use of proton MR spectroscopy: the limits of accuracy with a logistic regression model. AJNR Am J Neuroradiol 2000; 21:1213–1219.
28. Kizu O, Naruse S, Furuya S, et al. Application of proton chemical shift imaging in monitoring of gamma knife radiosurgery on brain tumors. Mag Reson Imaging 1998; 16:197–204.
29. Tate AR, Majòs C, Moreno A, Howe FA, Griffiths JR, Arús C. Automated classification of short echo time in in vivo ^{1}H brain tumor spectra: a multicenter study. Magn Reson Med 2003; 49:29–36.
30. Cirak B, Horska A, Barker PB, Burger PC, Carson BS, Avellino AM. Proton magnetic resonance spectroscopic imaging in pediatric pilomyxoid astrocytoma. Childs Nerv Syst 2005; 21:404–419.
31. Nafe R, Herminghaus S, Raab P, et al. Preoperative proton-MR spectroscopy of gliomas: correlation with quantitative nuclear morphology in surgical specimen. J Neurooncol 2003; 63:233–245.
32. Vuori K, Kankaanranta L, Hakkinen AM, et al. Low-grade gliomas and focal cortical developmental malformations: differentiation with proton MR spectroscopy. Radiology 2004; 230:703–708.
33. Tzika AA, Zarifi MK, Goumnerova L, et al. Neuroimaging in pediatric brain tumors: Gd-DTPA-enhanced, hemodynamic, and diffusion MR imaging compared with MR spectroscopic imaging. AJNR Am J Neuroradiol 2002; 23:322–333.
34. Castillo M, Smith JK, Kwock L. Correlation of myo-inositol levels and grading of cerebral astrocytomas. AJNR Am J Neuroradiol 2000; 9:1645–1649.
35. Rock JP, Hearsen D, Scarpace L, et al. Correlations between magnetic resonance spectroscopy and image-guided histopathology, with special attention to radiation necrosis. Neurosurgery 2002; 51:912–920.